

## Calculation of the hyperfine fields in the noble-metal atoms

R. W. Dougherty, Surya N. Panigrahy, and T. P. Das

*State University of New York at Albany, Albany, New York 12222*

J. Andriessen

*Technische Natuurkunde, Technische Universiteit Delft, 2628 CJ Delft, The Netherlands*

(Received 2 September 1992)

The hyperfine fields in the noble-metal atoms Cu, Ag, and Au have been calculated by means of a relativistic many-body perturbation-theory technique. The resulting hyperfine fields for these atoms were  $256 \pm 11$ ,  $531 \pm 22$ , and  $1997 \pm 92$  T, respectively, in good agreement with the experimental results of 259.95, 499.12, and 2085.1781 T. The reasons for the error bars in the theoretical results are discussed and are associated with the substantial sizes of the third- and higher-order correlation effects, which are found to be of great importance in these atoms. We will discuss the contributions to the total field from various one- and two-body interaction mechanisms and compare these contributions to those in related systems. Our results for the Cu and Au systems will also be compared with those available from other calculations reported in the literature.

PACS number(s): 31.30.Gs, 31.30.Jv, 31.20.Tz

### I. INTRODUCTION

In this paper, we present the results of our investigation of the hyperfine structures of the Cu, Ag, and Au atoms. Both the investigation of the present work and that of our previous work [1] on the closely related  $\text{Zn}^+$ ,  $\text{Cd}^+$ , and  $\text{Hg}^+$  ions were motivated primarily by a desire to understand the effect of the  $d$  shells and, in the cases of  $\text{Hg}^+$  and Au, the  $f$  shells on the hyperfine properties of these systems. The above systems would closely resemble either an alkali-metal atom or an alkaline-earth-metal ion were it not for the presence of these intervening  $d$  and  $f$  shells. Both the alkali-metal atoms [2] and the alkaline-earth-metal ions [3] have been studied in detail previously, and it is therefore possible to make comparisons between the corresponding systems. It is hoped that such comparisons would lead to a better understanding of all the systems. It is reasonable to expect electron correlation effects to be of greater relative importance as a function of the valence contribution in the noble-metal series and in the isoelectronic-ion series, because the extra  $d$  and  $f$  shells are expected to be more easily deformed by the electron-electron interactions as compared to the cores of the alkali-metal atoms, which are more compact and resemble the tightly bound inert gas atoms. This turns out not to be what is observed, however, because of the fact that there is a great deal of cancellation coming from correlation diagrams with different signs, leading to a relatively smaller net correlation contribution. One might also expect that exchange-core-polarization-(ECP) type effects may be of less relative importance because the additional shells would tend to shield the core  $s$  electrons, which make the major contribution to the ECP effects, from the exchange effects of the valence electron. This expectation turns out to be correct.

A few other calculations have been made earlier on some of these systems, using other techniques [4]. It was

our wish to compare our results with those of these other techniques, since we believe that such comparisons often lead to valuable insights concerning the methods involved. Finally, experimental measurements of the hyperfine fields in each of the noble metal atoms are available [5], so that one can judge the accuracy of our method.

Section II deals with a brief description of the procedure we have employed, and Sec. III presents our results, discussions, and conclusions from our investigations.

### II. PROCEDURE

The many-body technique we employ in these investigations has been described in a number of previous papers [6], and will only be briefly described here. Our calculation is carried out using a relativistic formalism, as we often deal with large atoms in which relativistic effects are important. The relativistic ground state of the system under study is first calculated by the restricted Hartree-Fock (RHF) method, which means that all electrons in a given shell are considered to have the same radial-wave function. The angular parts of the wave functions are those appropriate for a central field [7]. Excited single-particle wave functions are calculated in a  $V^{N-1}$  potential, that is, in a potential generated by all the occupied Hartree-Fock atomic states except one. We use these  $V^{N-1}$  states because they are known to be more physically meaningful than the Hartree-Fock (or  $V^N$ ) states [8], and perturbation expansions using these states converge more rapidly than expansions using the  $V^N$  states. We calculate discrete excited states with principal quantum number up to  $n = 12$ , and 15 states in the continuous spectrum with wave numbers corresponding to a Gauss-Laguerre integration formula [9].

The expectation value of the hyperfine operator is calculated over the many-electron wave function for the sys-

tem, including all the interactions within it, by means of a linked-cluster expansion [10]. Individual terms in this expansion may be represented by diagrams which may, in turn, be associated with real physical interactions. In practice, of course, one calculates the terms corresponding to diagrams that represent interactions which are expected to be significant. The rules for drawing diagrams and for translating [11] these diagrams into mathematical expressions will not be given here. We shall instead simply present the important diagrams that we have calculated and briefly explain their significance.

The diagram in Fig. 1(a) represents the zero-order approximation to the expectation value, which depends only upon the valence electron. The diagrams in Figs. 1(b)–1(e) represent the major effects of single-particle excitations. Figure 1(b) shows a core electron being excited due to its exchange interaction with the unpaired spin valence electron, after which it is scattered back into its original state by the hyperfine operator. This is the ECP effect. It serves as a correction to the assumption in the RHF approximation that all the electrons in a given shell have the same radial-wave function. This is obviously not the case, since only those core electrons with spins identical to that of the valence electron will experience exchange interactions with the unpaired spin valence electron. The diagram in Fig. 1(c) is a phase-space diagram related to the ECP diagram. It represents the effect of the scattering of core state electrons into the empty valence shell state. The diagrams in Figs. 1(d) and 1(e) represent typical higher-order corrections to the ECP diagram, and are referred to as EPV (exclusion-principle violating) and consistency diagrams, respectively. They are usually not found to be very significant in effect [6]. All the diagrams shown in Fig. 2 have two electrons excited simultaneously, and hence represent true many-body effects.

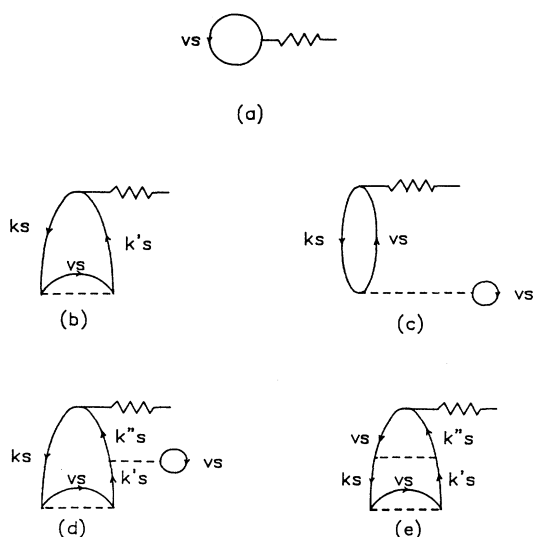


FIG. 1. Diagrams involving single-particle excitations. (a) Valence diagram. (b) ECP diagram. (c) Phase-space diagram. (d) and (e) are EPV and consistency diagrams, respectively, and act as second-order corrections to (b).

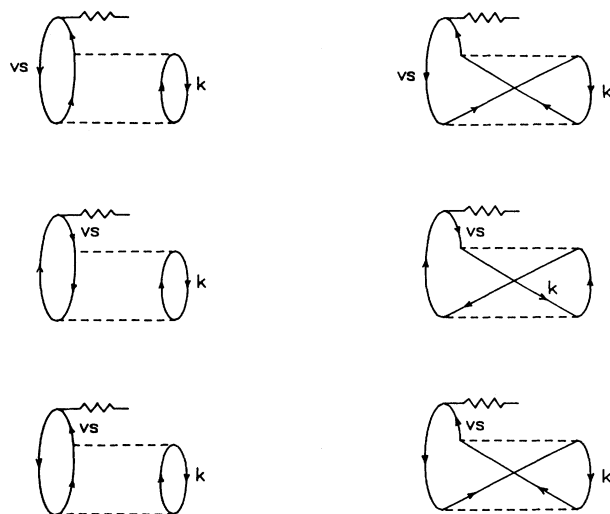


FIG. 2. The (0,2) correlation diagrams, both direct and exchange.

These are the so-called (0,2)-type correlation diagrams [10], and they provide the bulk of the correlation contribution to the expectation value. The (1,1) correlation diagrams are represented by the diagrams of Fig. 3. These are usually found to be less important than the (0,2) diagrams, but are often large enough to be significant [12]. It was found in our previous calculation on the  $\text{Zn}^+$ ,  $\text{Cd}^+$ , and  $\text{Hg}^+$  ions that the diagrams of Fig. 4 were also quite significant. These diagrams represent corrections to the expectation value over the many-body wave function produced by correlation between the electrons in the outermost  $d$  shell. Specifically, interactions between these electrons significantly alter the structure of the  $d$  shell, which requires the structure of the valence  $s$  shell to change in order to maintain self-consistency. These diagrams calculate the effect of this change in the valence shell on the expectation value. We have calculated a number of third- and fourth-order diagrams that represent this sort of effect; Fig. 4 gives only a few representative diagrams that are of significant magnitude.

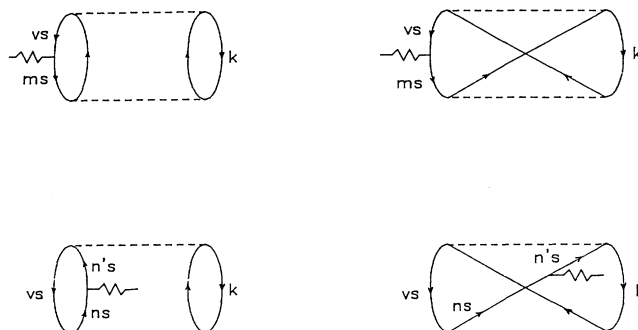


FIG. 3. The (1,1) correlation diagrams, both direct and exchange.

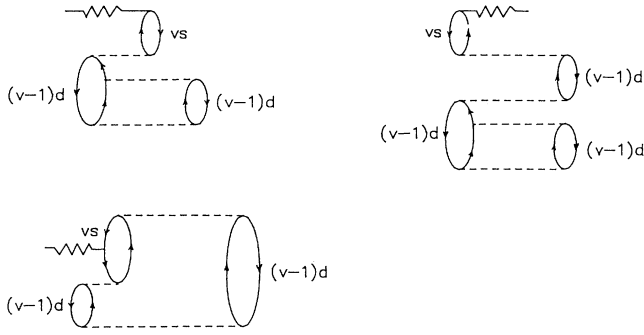


FIG. 4. Examples of high-order correlation diagrams.

The diagrams in Fig. 5 represent higher-order corrections to the correlation diagrams of Fig. 2. These diagrams may be evaluated easily by using a corrected energy denominator when calculating [13] the diagrams of Fig. 2. When this is done, the result is the sum of the contribution from the diagram in Fig. 2 and the corrections from the diagram in Fig. 5. This is what we have done, and hence the results we will be presenting for the second-order diagrams actually contain corrections for higher-order effects.

It should be noted that, when calculating diagrams, we have used the  $V^N$  hole wave functions and energy eigenvalues in place of the  $V^{N-1}$  hole states. By doing this, we include in the diagrams the effects of certain classes of higher-order corrections [14]. Also, the distribution of the magnetic moment of the nucleus may be of some significance for large nuclei. To account for this effect, we calculate our diagrams assuming the nuclear moment to be represented by a point magnetic-dipole moment, and multiply the result by a correction factor calculated according to a method due to Kopfermann and which we have utilized previously in a calculation for the  $\text{Ra}^+$  ion [15].

### III. RESULTS AND DISCUSSION

The main results of the calculation are presented in Table I, along with the available experimental results and the results of some other calculations. The results are listed in terms of the hyperfine field at the nucleus [16], so that they are independent of the magnetic moments of the isotopes, and are given in units of Tesla. This allows us to more effectively discuss trends between the atoms studied. The first line gives the zero-order contribution

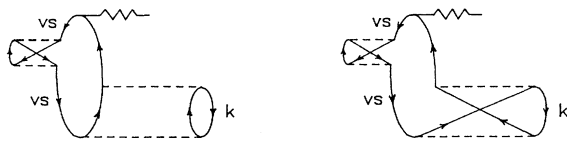


FIG. 5. Renormalization diagrams. These are evaluated by altering the energy denominators used to evaluate the (0,2) correlation diagrams.

TABLE I. Breakdown of the contributions (in T) to the hyperfine fields in the noble-metal atoms by various one- and two-body mechanisms.

Contribution	Cu	Ag	Au
Valence	178.05	366.32	1527.33
ECP plus phase space	21.04	41.14	148.78
EPV plus consistency	8.43	14.59	78.49
Second-order correlation	50.24	119.78	280.20
Higher-order correlation	-2.18	-11.26	-37.49
Total	256±11	531±22	1997±92
Experiment	259.95 <sup>a</sup>	499.12 <sup>b</sup>	2085.1781 <sup>b</sup>
Other calculations	258.19 <sup>c</sup>		2074.5108 <sup>d</sup>

<sup>a</sup>Reference [5(a)].

<sup>b</sup>Reference [5(b)].

<sup>c</sup>Reference [4(a)].

<sup>d</sup>Reference [4(b)].

to the field that, as mentioned before, is entirely due to the valence electron. The second line gives the contribution to the field from the ECP and phase-space diagrams of Figs. 1(b) and 1(c). The phase-space diagram typically gives a much smaller contribution than the ECP diagram, because only a single state (the spin-down state in the valence shell) is available as an excited state. The third line gives the contributions from all the EPV and consistency diagrams. Figures 1d and 1e are typical diagrams of this type, although other diagrams in this family have also been evaluated. These latter two lines are grouped together because they represent contributions from terms in which only a single particle is excited. The fourth line gives the contribution from the (0,2)- and (1,1)-type correlation diagrams of Figs. 2 and 3. It should be remembered, however, that the energy denominators appearing in the expressions for these diagrams have been altered so that the contributions of the diagrams of Fig. 5 are also included in this result. The fifth line gives the contribution of the higher-order correlation diagrams, both those of Fig. 4 and some others. The sixth line displays the total hyperfine field, the seventh line gives the results from experimental observations, and the last gives the results of some previous calculations.

We will now consider the contributions from the one- and two-electron excitation mechanisms in some detail. Table II displays the contributions of individual core  $s$

TABLE II. Contributions (in T) of various core shells to the ECP plus phase-space part of the hyperfine field.

Shell	Cu	Ag	Au
1s	3.14	3.00	4.34
2s	4.58	4.68	10.10
3s	13.32	8.32	14.88
4s		25.14	28.27
5s			91.19
Total	21.04	41.14	148.78

TABLE III. Contributions (in T) of various core shells to the (0,2) correlation contribution to the hyperfine field.

Shell	Cu	Ag	Au
$(V-1)s$	0.63	1.90	5.35
$(V-1)p$	4.08	10.61	35.20
$(V-1)d$	48.24	117.49	262.98
$(V-1)f$			43.80
Total	52.95	130.00	347.33

shells to the sum of the ECP and phase-space diagrams. Table III gives the contributions of the outermost core shells to the (0,2) correlation contribution. Table II shows that the ECP plus phase-space contributions of the core shells decrease rapidly as one goes deeper into the core. This has been observed before [17], and may be explained quite easily. The deeper core shells are more isolated from the valence electron and thus have weaker exchange interactions with it. They also have higher excitation energies as well. Both of these facts would tend to decrease their contributions. Their greater spin density at the nucleus obviously does not overcome this effect. In Table IV, we display the ratios of the total one- and two-electron excitation contributions to the valence contribution. We see from the second line of Table IV that there is a slow decrease in the ratio of the sum of the one-electron contributions (which will be referred to as the net ECP contribution, since they are all related to the way core electrons with differing spins interact with the unbalanced spin of the valence electron) to the valence contribution as one goes from Cu to Au. This also has been seen before for the alkali-metal atoms [2], the alkaline-earth-metal ions [3], and the  $Zn^+$ ,  $Cd^+$ , and  $Hg^+$  ions, which are isoelectronic with the noble-metal atoms [1]. As the nuclear charge increases, the core shells contract. This tends to increase the shielding effect on the nuclear charge, and consequently the valence shell tends to expand and become more deformable. The greater distance between the valence and the core electrons, and the higher excitation energies for the cores, result in the observed decrease in the ratio. As in the isoelectronic-ion systems, the magnitudes of the ratios are believed to be smaller than in the alkali-metal atoms because of the presence of the extra intervening  $d$  shells (and the  $f$  shell in Au), which tend to separate the valence and inner-core shells. The ratios are larger in the current systems than in the isoelectronic-ion systems because the current systems are electrically neutral, and thus excitations of all kinds are more likely because the systems are less tightly bound.

TABLE IV. Ratios (in %) of the Net ECP and total correlation contributions to the valence contributions of the hyperfine fields.

Ratio	Cu	Ag	Au
Net ECP <sup>a</sup> :valence	16.6	15.2	14.9
Correlation:valence	27.0	29.6	15.9

<sup>a</sup>Refers to the total contribution of all one-electron mechanisms.

Table III shows that the leading (0,2) correlation contribution comes, in all cases, from correlation with the outermost  $d$  shell, as would be expected both from physical considerations involving the greater deformability of the  $d$  shells as compared to the others and from the calculations on the isoelectronic systems. It is surprising that the next largest contribution for the Au system is the  $f$  shell, as this was not the case for the isoelectronic  $Hg^+$  ion. Apparently this shell contracts significantly in  $Hg^+$  when the effective charge is increased to unity from zero in Au. The second largest contributor for the Cu and Ag systems is the outermost  $p$  shell, followed by the outermost  $s$  shell. In Au, these shells are the third and fourth largest contributors, respectively. This order is easily explicable in terms of interelectronic interaction strengths and excitation energies, as above. The ratios of the total correlation contributions to the valence contributions are shown in Table IV. It is seen that, as one goes down the periodic table, there is first a small rise in the ratio, then a major decrease. This trend is similar to that found in the alkali-metal atoms [2], but different from that in the isoelectronic-ion systems [1], which displayed a monotonic decrease. The observed trend in the present systems is believed to result from competition between the effects of the increasing deformability of the valence shell and its increasing distance from the core, due to the reasons mentioned above in explaining the ECP contributions. In the case of the isoelectronic-ion systems, it appears that the influence of the increasing distance between the core and valence electrons wins out, leading to the observed monotonic decrease from  $Zn^+$  to  $Hg^+$ . The magnitudes of the ratios are, in the present neutral atomic systems, considerably larger than in the isoelectronic-ionic systems. This is also a result of the fact that these systems are less tightly bound because of their neutrality, and thus there is considerably more correlation.

As was the case in our previous calculation on the isoelectronic ions  $Zn^+$ ,  $Cd^+$ , and  $Hg^+$ , one of the important features of this calculation is found in the fifth line of Table I, that is, in the contributions from the third- and higher-order correlation diagrams. This contribution ranges from just over 1% of the valence contribution for Cu, to about 2.5% in the Au system, and about 3% of the valence contribution for Ag. In all three cases, the proportion is relatively high compared to other systems with single electrons in the valence shell (such as the alkali-metal atoms, for instance), indicating that there is significant correlation among the outermost  $d$ -shell electrons, and that the valence electron is sensitive to this correlation. Also, a great deal of cancellation was observed among the diagrams that are represented on this line, the sum being the results of larger numbers with differing signs being added together. Finally, a complete fourth-order calculation is not practical because of the large number of diagrams involved, and only the ones expected to make leading contributions are included in our calculation of these higher-order effects. Because of the above facts, and because of limitations in computational accuracy, we ascribe a conservative confidence limit of 6% of the valence contribution to our calculation, a value

significantly larger than those appearing in related systems [1,2].

In comparing the total field obtained in this calculation with the experimental results [5] and with the results of the other calculations [4] for Cu and Ag, it may appear that the other calculations are in better agreement with the experimental results. We believe that there are some uncertainties in the other calculations. Specifically, the calculation of Ref. [4(a)] for the Cu atom used a differential-equation technique that probably could not take the (1,1) diagrams of Fig. 3 into account [6(i)]. The calculation of Ref. [4(b)] for the Au atom not only failed to include these same diagrams, but also ignored the renormalization diagrams of Fig. 5 and the effects of the distribution of the nuclear magnetic moment. The (1,1) correlation diagrams contribute approximately  $-10$  T to the current calculation for Cu, and would probably give a similar contribution to the results of the calculation of Ref. [4(a)], thereby reducing its agreement with the experimental result. When the (1,1) correlation diagrams, renormalization diagrams, and magnetization distribution effects are removed from the current calculation, the final result for Au is increased by about 160 T; it is

reasonable to conclude that the addition of these effects to the calculation of Ref. [4(b)] would produce a decrease of a similar amount, to about 1960 T, thereby weakening the apparent agreement between Ref. [4(b)] and experiment.

In summary, we have calculated the hyperfine fields in the Cu, Ag, and Au atoms and achieved good agreement with the experimental results. We have, however, found that higher-order correlation effects are extremely important in these systems, and because of this, we assign a larger confidence limit to our results than has been used for other classes of atomic systems with single valence electrons.

#### ACKNOWLEDGMENT

This research was conducted using the Cornell National Supercomputer Facility, a resource of the Center for Theory and Simulation in Science and Engineering at Cornell University, which is funded in part by the National Science Foundation, New York State, and the IBM Corporation.

- 
- [1] Surya N. Panigrahy, R. W. Dougherty, T. P. Das, and J. Andriessen, *Phys. Rev. A* **44**, 121 (1991).
- [2] (a) Mina Vajed-Samii, S. N. Ray, and T. P. Das, *Phys. Rev. A* **20**, 1787 (1979); (b) Mina Vajed-Samii, J. Andriessen, B. P. Das, S. N. Ray, T. Lee, and T. P. Das, *J. Phys. B* **15**, L379 (1982).
- [3] S. Ahmad, J. Andriessen, K. Raghunathan, and T. P. Das, *Phys. Rev. A* **25**, 2923 (1982); S. Ahmad, J. Andriessen, and T. P. Das, *ibid.* **27**, 2790 (1983).
- [4] (a) J.-L. Heully, *Z. Phys. A* **319**, 253 (1984); (b) S. Ahmad, *J. Phys. B* **17**, L807 (1984).
- [5] (a) H. Figger, D. Schmitt, and H. Penselin, in *La Structure Hyperfine Magnétique des Atomes et des Molécules*, edited by R. Lefebvre and C. Moser (CRNS, Paris, 1966); (b) H. Dahmen and S. Penselin, *Z. Phys.* **200**, 456 (1967).
- [6] (a) E. S. Chang, R. T. Pu, and T. P. Das, *Phys. Rev.* **174**, 1 (1968); (b) N. C. Dutta, C. Matsubara, R. T. Pu, and T. P. Das, *Phys. Rev. Lett.* **21**, 1139 (1968); (c) *Phys. Rev.* **177**, 33 (1969); (d) T. Lee, N. C. Dutta, and T. P. Das, *Phys. Rev. A* **1**, 995 (1970); (e) J. Andriessen, K. Raghunathan, S. N. Ray, and T. P. Das, *Phys. Rev. B* **15**, 2533 (1977); (f) Mina Vajed-Samii, J. Andriessen, S. N. Ray, and T. P. Das, *Phys. Rev. A* **20**, 1787 (1979); (g) Mina Vajed-Samii, J. Andriessen, B. P. Das, S. N. Ray, and T. P. Das, *Phys. Rev. Lett.* **48**, 1330 (1982); **49**, 180 (1982); **49**, 1466 (1982); (h) Surya N. Panigrahy, R. W. Dougherty, T. P. Das, and J. Andriessen, *Phys. Rev. A* **40**, 1765 (1989); (i) Surya N. Panigrahy, R. W. Dougherty, S. Ahmad, K. C. Mishra, T. P. Das, J. Andriessen, R. Neugart, E. W. Otten, and K. Wendt, *ibid.* **43**, 2215 (1991).
- [7] I. P. Grant, *Proc. R. Soc. London, Ser. A* **262**, 555 (1961).
- [8] T. P. Das, *Hyperfine Interactions* **39**, 149 (1987); E. S. Chang, R. T. Pu, and T. P. Das, *Phys. Rev.* **176**, 16 (1968).
- [9] A. H. Stroud and Don Secrest, *Gaussian Quadrature Formulas* (Prentice-Hall, Englewood Cliffs, NJ, 1966).
- [10] E. S. Chang *et al.*, Ref. [6(a)]; Surya N. Panigrahy *et al.*, Ref. [6(i)].
- [11] E. S. Chang *et al.*, Ref. [6(a)].
- [12] Surya N. Panigrahy *et al.*, Ref. [6(i)].
- [13] J. Andriessen, S. N. Ray, Taesul Lee, Dennis Ikenberry, and T. P. Das, *Phys. Rev. A* **13**, 1669 (1976); J. Andriessen, K. Raghunathan, S. N. Ray, and T. P. Das, *Phys. Rev. B* **15**, 2533 (1977).
- [14] Attaching passive interactions with the excluded state to the  $V^{N-1}$  state turns that state into the corresponding  $V^N$  state.
- [15] H. Kopfermann, *Nuclear Moments* (Academic, New York, 1958), p. 123; Ref. [6(i)].
- [16] Mina Vajed-Samii *et al.*, Ref. [2(b)].
- [17] Mina Vajed-Samii *et al.*, Ref. [2(b)]; Surya N. Panigrahy *et al.*, Ref. [1]; S. Ahmad *et al.*, Refs. [2(a)] and [2(b)].